frontiers | Frontiers in Marine Science

TYPE Original Research
PUBLISHED 03 October 2023
DOI 10.3389/fmars.2023.1215567

OPEN ACCESS

EDITED BY
Aldo Cróquer,
The Nature Conservancy,
Dominican Republic

REVIEWED BY
Tali Mass,
University of Haifa, Israel
Francisca C. García,
King Abdullah University of Science and Technology, Saudi Arabia
Esteban Agudo-Adriani,
University of North Carolina at Chapel Hill, United States

*CORRESPONDENCE
Na'ama-Rose Kochman-Gino
nr.kochman@gmail.com

RECEIVED 02 May 2023
ACCEPTED 11 September 2023
PUBLISHED 03 October 2023

CITATION
Kochman-Gino N-R and Fine M (2023) Reef building corals show resilience to the hottest marine heatwave on record in the Gulf of Aqaba.
Front. Mar. Sci. 10:1215567.
doi: 10.3389/fmars.2023.1215567

Reef building corals show resilience to the hottest marine heatwave on record in the Gulf of Aqaba

Na'ama-Rose Kochman-Gino[1,2]* and Maoz Fine[1,2]

[1]Department of Ecology, Evolution and Behavior, The Alexander Silberman Institute of Life Sciences, The Hebrew University of Jerusalem, Jerusalem, Israel, [2]The Interuniversity Institute for Marine Sciences, Eilat, Israel

Coral reefs are facing rapid deterioration, primarily due to a global rise in seawater temperature. In conjunction, the frequency and intensity of extreme high temperature events, known as marine heatwaves (MHWs), are increasing. The Gulf of Aqaba (GoA) in the northern Red Sea is home to corals known for their thermal resilience, yet concerns have been raised regarding the potential for MHWs to put this coral refuge at risk. In summer of 2021, the hottest MHW so far occurred in the GoA, with sea surface temperatures peaking at 31°C and persisting above the local summer maximum for 34 days. To assess the physiological response of the corals *Stylophora pistillata* and *Pocillopora damicornis* to this event, we analyzed the monthly content across a year of host and symbiont proteins, carbohydrates, and lipids, pre-, during, and post the MHW, as a proxy for metabolic stress. We found that the MHW was not fatal to either species and did not induce bleaching, based on algal densities and chlorophyll content. Species-specific responses were detected. In *S. pistillata*, host protein content decreased (33%) at the onset of the MHW (August) compared to pre-MHW levels (July). Algal symbionts of *S. pistillata* were unaffected by the MHW in their maximal photosynthetic efficiency (*Fv/Fm*) and exhibited higher carbohydrate levels (+34%) at the end of the MHW (September) compared to its onset. In contrast, no significant catabolic response was detected in *P. damicornis* host or symbionts, and the maximal relative electron transport rate (rETRmax) of symbionts was 37% higher during the MHW than the annual average. These results highlight the remarkable ability of common GoA corals to withstand extreme thermal anomalies, underscoring the global significance of this coral refuge.

KEYWORDS

marine heatwave, Stylophora pistillata, Pocillopora damicornis, coral reef, Gulf of Aqaba, coral reef refuge

1 Introduction

Coral reefs are among the most productive and biodiverse ecosystems, which support more than half a billion people as a source of food, medicinal compounds, provide coastal protection, and income from tourism and fisheries (Hoegh-Guldberg, 2011). However, coral reefs are rapidly deteriorating due to anthropogenically induced, global, and local factors (Hoegh-Guldberg et al., 2007; Hughes et al., 2017; Eddy et al., 2021), which have a deleterious synergistic effect (Donovan et al., 2021). Rising seawater temperatures pose the most immediate threat to coral reefs worldwide (Hughes et al., 2018). Corals often bleach when exposed to 1-2˚C above the local summer maximum (LSM) temperature (Hoegh-Guldberg, 1999) and may die as a result of depletion in photosynthetic products and starvation (Szmant and Gassman, 1990; Grottoli et al., 2004).

In conjunction with the consistent long-term warming, there is an increase in the intensity and frequency of extreme temperature events known as marine heatwaves (MHWs; Hobday et al., 2016; Oliver et al., 2018). MHWs are periods of at least five days of temperature above the 90th percentile of the long-term observed values in a given location during the same time of the year (Hobday et al., 2016). MHWs are characterized by their intensity (I_{max}= Maximum temperature above the climatological mean), onset rate (R_{onset}= rate of heating from peak intensity to climatological mean), and duration (I_{cum}= the sum of daily anomalies above the climatological mean; Hobday et al., 2016).

Although long-term seawater temperature rise and acute MHWs both result in coral bleaching and consequent mortality, Fordyce et al. (2019) demonstrated graver physiological outcomes in corals during MHWs. In comparison to long-term thermal anomalies (DHW>8), corals under MHWs suffer from widespread tissue necrosis (which often precedes bleaching), widespread mass mortality coupled with fewer chances of recovery, and slower planulae recruitment (Fordyce et al., 2019). Following a MHW at Heron Island (southern Great Barrier Reef, Australia) in March 2020, significant declines in hard coral cover were reported (Brown et al., 2023). In 2019, a severe MHW in Moorea (French Polynesia) resulted in widespread size-dependent coral mortality, as high-percentage mortality of the largest *Pocillopora* and *Acropora* colonies was recorded (Speare et al., 2022). The disproportional mortality of large colonies diminished the fecundity of *Pocillopora* and *Acropora* genera by more than 60% (Speare et al., 2022). During a MHW in Hawai'i (USA) in 2019, bleaching-resistant and bleaching-susceptible phenotypes of *Montipora capitata* and *Pocillopora compressa* significantly reduced their metabolic rate and photochemical capacity (Innis et al., 2021). The outcomes of the aforementioned events and others (Shlesinger and van Woesik, 2023) are troubling due to the projections that by 2100, MHWs will occur nearly everywhere, regardless of possible variations in emissions scenarios (Frölicher et al., 2018). Hence, it was suggested that the more frequent MHWs would push marine ecosystems beyond their resilience limits (Frölicher et al., 2018).

Corals of the Gulf of Aqaba (GoA), located in the northern Red Sea, are known for their thermal resilience (Fine et al., 2013; Bellworthy and Fine, 2017; Grottoli et al., 2017; Krueger et al., 2017; Osman et al., 2018; Kochman et al., 2021). No mass bleaching event was recorded in the northern Red Sea (Osman et al., 2018). Furthermore, common GoA coral species do not bleach when experimentally exposed to 1-2˚C above the LSM (27.5˚C; Bellworthy and Fine, 2017; Krueger et al., 2017; Kochman et al., 2021) and can withstand up to 32˚C, +5˚C above the LSM (Fine et al., 2013). In *in-situ* and experimental studies proposed that the GoA may serve as a potential coral refuge from climate change until the end of the century (Fine et al., 2013; Osman et al., 2018; Kleinhaus et al., 2020).

While northern Red Sea reefs show high thermal resistance (Fine et al., 2013), the predicted higher frequency of MHWs in the northern Red Sea raised concern as to its potential to serve as a coral refuge (Genevier et al., 2019). While there were no recordings of MHWs in the GoA until 2015 (Genevier et al., 2019), in July 2017, two consecutive MHWs with exceptionally high onset rates occurred. During the first event, thermally stressed fish belonging to dozen of species died (Genin et al., 2020). This was explained by the increased virulence of a pathogenic *Streptococcus iniae*, triggered by the rapid onset of the MHWs, rather than the peak temperature (Genin et al., 2020). No visible bleaching or coral mortality was seen in the reef during the same period (Israel National Monitoring Program of the Gulf of Eilat, 2017). In August 2021, the hottest MHW on record occurred in Eilat, with SST (sea surface temperature) reaching 31˚C (Israel National Monitoring Program of the Gulf of Eilat, 2021). The onset rate of the MHW was milder than in 2017, yet of higher intensity and duration. Nevertheless, no mass fish mortality or coral bleaching was reported during the MHW of 2021 (Israel National Monitoring Program of the Gulf of Eilat, 2021).

Although coral bleaching is the most distinct symptom of thermal stress, higher than optimum temperatures (in which an organism has the greatest synchronization of molecular, cellular, and systemic processes; Pörtner and Farrell, 2008) can trigger benign but life-preserving metabolic processes in the coral host, while the association of the host-algae remains intact (Rädecker et al., 2021). Innis et al. (2021) demonstrated pronounced metabolic depression even in bleaching-resistant corals during a MHW in Hawai'i (2021). While lowering metabolic rates allows short-term survival, it may have deleterious effects on the ecological success and energetic status of the coral holobiont in the long term (Pörtner and Farrell, 2008), and consequently reduced feeding (Ferrier-Pagès et al., 2010), calcification rates (Cantin and Lough, 2014), and reproduction output (Baird and Marshall, 2002).

While coral physiology under climate change scenarios in the GoA is well-studied (Fine et al., 2013; Bellworthy and Fine, 2017; Krueger et al., 2017; Kochman et al., 2021), as well as their response to short-term thermal anomalies (Evensen et al., 2021; Savary et al., 2021), an ecologically-relevant, *in-situ* assessment to the frequent and intensifying MHWs is lacking. Understanding how thermally resistant corals respond to a naturally occurring MHW will shed light on their capacity to endure future ocean conditions. In this study, we examined the monthly physiological response of two common, branching coral species across a year, encompassing a category II (strong) MHW (*sensu* Hobday et al., 2018), while focusing on changes in host and symbiont energy reserves as a proxy for metabolic stress.

2 Materials and methods

2.1 Environmental conditions

The maximal daily temperature (Figure 1A) was computed by extracting and averaging the maximal daily temperatures measured from 2-m depth, 50-m from the sampling site, from the website of the National Monitoring Program (NMP) of the Gulf of Eilat (Israel National Monitoring Program of the Gulf of Eilat, 2021). The long-term climatology data for the characterization of the MHW (*sensu* Hobday et al., 2018; Section 2.4) consisted of daily temperature from August 1st until September 5th of the last 33 years (1988-2021), since measurements began near the Inter-university Institute (IUI) for Marine Sciences in Eilat, Israel. These dates were chosen since they led to bleaching alert area 3 and 8- degrees heating weeks (NOAA, 2021).

Averaged monthly seawater temperature during this study (2021-2022), the 10-year (2011-2021) and the 30-year average (1991-2021) are presented in Figure 1B. Daily temperature was extracted (NOAA, 2021) by averaging the daily max and min sea surface temperatures using satellite imagery, and the average monthly temperature was calculated.

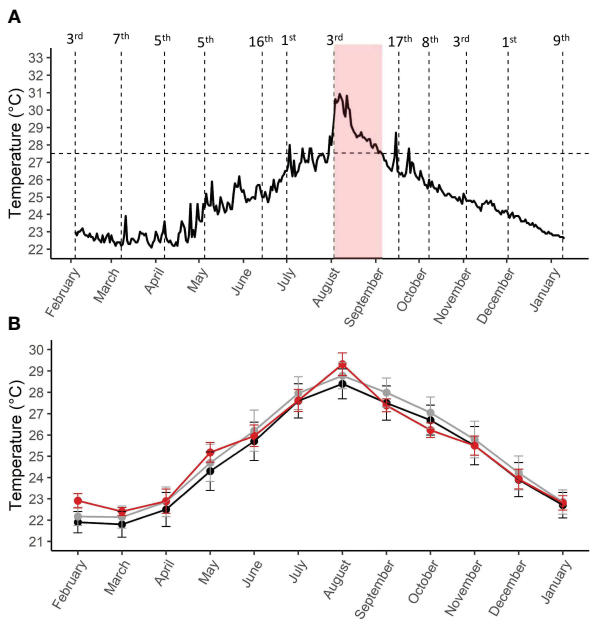

FIGURE 1
(A) Maximal daily temperature from February 2021 to January 2022 (Israel National Monitoring Program of the Gulf of Eilat, 2022). Horizonal line indicates the monthly mean maximum of Eilat (27.5°C, NOAA). Sampling dates are specified above the vertical dashed lines. The shaded red area denotes the marine heatwave. **(B)** Averaged monthly temperature, based on NOAA coral reef watch for the Gulf of Aqaba (NOAA, 2021). The 30-year average of years 1991-2021 (in black), the 10-year average of years of 2011-2020 (gray), and the experimental period of 2021-2022 (in red). Error bars are standard deviations.

2.2 An in-situ, monthly assessment of coral and symbiont physiology before, during and after a marine heatwave

Eight tagged *Stylophora pistillata* and *Pocillopora damicornis* parent colonies (23 ± 4 cm and 21 ± 2.5 cm radius, respectively) were sampled monthly (surface area of 4.5 ± 2.6 cm^2) with a cutter into an individual ziplock bag from February 2021 until January 2022 (n=1 fragment per parent-colony) from the coral nursery of the IUI (29°30'N, 34°55'E). The sampled coral colonies were collected in different locations along Eilat's coast. Therefore, it is unlikely that these colonies are genetically identical. All parent colonies were maintained at a depth of ~7 m. Overall, 192 coral nubbins were sampled. Given the large size of the parent colonies and the small fragment number and size, it was assumed that the repeated sampling did not cause significant stress to the colonies. Sampling dates were apart by 31 ± 9 days (Figure 1A).

The two examined branching coral species are of the family *Pocilloporidae*. Both have small polyps, are thermally resistant in the GoA (with *P. damicornis* considered more thermally resistant; Grottoli et al., 2017), and are mainly autotrophic (Alamaru et al., 2009; Tremblay et al., 2016; Dobson et al., 2021). *S. pistillata* shallower than 17 m hosts mainly *Symbiodinium* algal symbionts (Lampert-Karako et al., 2008; Byler et al., 2013), while *P. damicornis* harbors *Cladocopium* in the northern GoA (Karako-Lampert et al., 2004).

2.2.1 Pulse amplitude modulated fluorometry

Following 20-minute dark acclimation (Jones et al., 1998; Hoegh-Guldberg and Jones, 1999; Warner et al., 1999), the collected coral nubbins were exposed to rapid light curves (RLC; Ralph and Gademann, 2005) to assess the quantum yield of photosystem II (PSII) to increasing PAR (0 to 701 µmol photons m^{-2} s^{-1}), using an Imaging-PAM (I-PAM, Walz, GmbH, Effeltrich, Germany). Maximal quantum yield (F_v/F_m) was computed by F_m-F_o/F_m, as F_m and F_0 are the maximal and minimal fluorescence, respectively, following the dark acclimation. Relative electron transport rate (rETR) was calculated as Y(II)*PAR*0.5 (Ralph and Gademann, 2005). Maximal rETR ($_rETR_{max}$) is the maximal rate for each nubbin. A curve of rETR by PAR was generated for each sample using R (version 3.6). Photosynthetic efficiency (alpha) was calculated as the slope of the curve in light-limiting irradiance. Saturating irradiance (iK) was computed by iK= rETRmax/alpha. Reduced Fv/Fm, rETRmax, alpha, and iK values suggest malfunctioning photosystem II.

Measurements for *P. damicornis* in December 2021 were not performed due to technical issues. Following chlorophyll fluorescence measurements, the nubbins were flash-frozen and kept at -80°C until further processing.

2.2.2 Algal density and chlorophyll content

Tissue of the coral nubbins was blasted off using an airbrush into 5 ml of ice-cold PBS (pH 7.4, Sigma-Aldrich) and was then homogenized manually using a mortar and a pestle.

Algal density subsamples (96 µl) were fixed using 4% formaldehyde and then counted by a fluorescent cell counter (DeNovix CellDrop FL; Pi, 40µl, n=4/sample).

Chlorophyll subsamples (1 ml) were centrifuged (Sigma 4K15, 5000 rpm, 5 min, 4˚C), the supernatant discarded, and the chlorophyll in the pellet extracted (1 ml of 100% acetone, 24-h incubation in 4˚C). Extracts were loaded in triplicates in acetone-resistant plates, and their absorbance was read in a spectrophotometer (Biotek HT Synergy). Chlorophyll content was calculated based on Jeffrey and Humphrey (1975).

Algal density and host macromolecules (proteins, carbohydrates, lipids) were normalized by the surface area of the dry coral skeleton using the single wax dipping method (Veal et al., 2010). Chlorophyll and the macromolecules of the algal symbionts were normalized by the algal cell count.

2.2.3 Proteins, carbohydrates, lipids, and total energy

A subsample of tissue slurry was centrifuged (1 ml; 700 g, 10 min, 4˚C) to separate fractions of the coral host and algal symbiont. The supernatant was kept as a host fraction. The algal pellet was washed in PBS, centrifuged (700 g, 5 min, 4˚C), and resuspended in 1 ml PBS. Later, the symbiont fraction was sonicated (ultrasonic cleaner, DCG-120H, MRC, 10 min, 4˚C) to break the algal cells. The proteins, carbohydrates, and lipids content were determined for both host and symbiont fractions of every sample. Macromolecule assays were conducted as in Kochman et al. (2021). Briefly, proteins were quantified using the improved Bradford method (Zor and Selinger, 1996), as Bovine Serum Albumin served as a standard, and reading in a spectrophotometer (Biotek HT Synergy; 450 and 595 nm).

Carbohydrates were determined using the Sulphuric acid-phenol method, with glucose as the standard (Masuko et al., 2005) and reading in a spectrophotometer (Biotek HT Synergy; 490 nm).

Lipids content was determined by the sulphu-phospho-vanillin assay, with corn oil as standard (Cheng et al., 2011) and reading in a spectrophotometer (Biotek HT Synergy; 540 nm).

Total energy was calculated by multiplying the content of each macromolecule by its relative combustion enthalpy (Gnaiger and Bitterlich, 1984) and then summing them (Grottoli et al., 2017). Total energy includes structural and stored macromolecules, yet structural lipids can be used as reserves under stressful conditions in corals (Rodrigues et al., 2008; Imbs and Yakovleva, 2012). To improve accuracy, total energy consists of values not identified as outliers in any specific macromolecule.

2.3 Excursion of physiological parameters from seasonal range during the MHW

The effects of the MHW can be better interpreted for every parameter while considering the excursion from the seasonal range (anomaly; Tables 1, 2). The seasonal range includes the average monthly maximum and minimum values, excluding values in August- during the peak of the MHW. Therefore, if values in August are beyond the seasonal range, differ from the annual average, and are significantly different from the adjacent months, it may suggest a physiological effect induced by the MHW.

2.4 Simulated marine heatwave analysis

Thermal stress scenarios in Kochman et al., 2021 were categorized following Hobday et al., 2018 (see section 4). The 31-year climatology and its 90th percentile were calculated (Israel National Monitoring Program of the Gulf of Eilat, 2017). An average delta between the climatology and the 90th percentile of the climatology was computed. This delta (threshold) and its multiples (X2, X3, X4, X5) were plotted and were used to determine the maximum intensity of the simulated marine heatwaves, of 31˚C and 33˚C for 10 days, with an Ronset= +1˚C/day. The marine heatwave was categorized as more severe as it crossed a higher threshold.

2.5 Statistical analysis

Raw data was visualized to evaluate the distribution and examine potential outliers. Then, for each dependent variable in each species, a linear mixed effects model was performed (lmer, R package: {lme4}; Bates et al., 2014), with the fixed factor "month" and the random factor "parent colony". Species were not tested as a fixed factor in the model, since the values between species were distinctly different in most parameters. P-values and F-statistics (Table 3) were achieved using the command "anova" (anova, R package: {stats}). The impacts of the fixed and random factors on the model fit were calculated using the r.squaredGLMM function (R package: {MuMIn}((Barton, 2020))). The proportion of variance explained by the fixed factors only is denoted by the marginal R^2 value, while the proportion of variance described by random and fixed factors is the conditional R^2 value, thus enabling the detection of colony effects. Equal variance and normal distribution of residuals were tested as model assumptions. If these were met and the results of the model were significant (p-value < 0.05), Tukey *post-hoc* was conducted to determine which of the months were significantly different (lsmeans, R package: {emmeans}, adj = ``tukey" (Lenth et al., 2018). PERMANOVA were performed if model assumptions were violated (adonis, R package: {vegan}) (Oksanen, 2007)). All graphics and statistical tests (R package: {ggplot2}(Wickham, 2016)) were generated in Rstudio version 3.6 (https://www.r-project.org/; R Core Team, 2020).

3 Results

3.1 Environmental conditions

In summer 2021, a category II MHW occurred in the reef of Eilat, GoA (Figure 1A) with an onset rate of 3.2˚C over five days (Maximum temperature above the climatological mean (I_{max})=3.5˚C, mean temperature above climatological mean (I_{mean})=1.9 ˚C, the sum of

TABLE 1 Seasonal variation (averaged maximum and minimum monthly values, excluding August), and averaged values during the MHW (August) ± STD in *Stylophora pistillata*.

	Seasonal range	MHW average
Algal density (Cells cm^{-2})	5.7 ± 2.12*10^6 (Jan)-2.6*10^6 ± 6.8*10^5 (Dec)	2.3*10^6± 6.3*10^5
Chlorophyll (pg $cell^{-1}$)	2 ± 0.2 (Jan)- 1.2 ± 0.2(Jun)	1.4 ± 0.3
Fv/Fm	0.62 ± 0.03 (Dec)- 0.54 ± 0.03 (Feb)	0.62 ± 0.02
rETRmax	44.11 ± 10.8 (Sep)- 15.43 ± 1.81 (Jan)	32.97 ± 9.26
iK	10.2 ± 1.41(Sep)- 3.46 ± 0.42 (Dec)	6.50 ± 1.55
Alpha	5.11 ± 0.28 (May)- 3.97 ± 0.43 (Nov)	5.11 ± 0.3
Host proteins (mg cm^{-2})	1.7 ± 0.7 (May)- 1.2 ± 0.2 (Nov)	1.1 ± 0.4
Host carbohydrates (mg cm^{-2})	0.33 ± 0.12 (Apr)- 0.15 ± 0.07 (Dec)	0.16 ± 0.05
Host lipids (mg cm^{-2})	0.71 ± 0.36 (Dec)- 0.29 ± 0.23 (Oct)	0.29 ± 0.24
Host total energy (J cm^{-2})	69.71 ± 25.19 (May)- 47.28 ± 14.52 (Oct)	38.14 ± 15.34
Symbiont proteins (pg $cell^{-1}$)	44.62 ± 11.4 (Sep)– 30.63 ± 21.49 (Feb)	44.25 ± 12.0
Symbiont carbohydrates (pg $cell^{-1}$)	29.76 ± 3.71 (Mar)- 18.97 ± 3.71 (Nov)	20.07 ± 1.39
Symbiont lipids (pg $cell^{-1}$)	59.83 ± 46.56 (Jul)- 21.7 ± 22.98 (May)	35.38 ± 21.64
Symbiont total energy (µJ $cell^{-1}$)	3.01±-0.78 (Jul)- 2.14 ± 1.19 (Feb)	2.46 ± 0.65

daily anomalies above the climatological mean (I_{cum})=70, rates of heating and cooling from peak intensity to climatological mean (R_{onset} and $R_{decline}$=0.3). Sea surface temperature (SST) peaked at 31˚C (+3.5˚C above the LSM of 27.5˚C; Israel National Monitoring Program of the Gulf of Eilat, 2021), making it the warmest MHW on record in the northern Gulf of Aqaba. This temperature anomaly (Figure 1B; Supplementary Figure 1) persisted for 34 days, reaching 8˚-heating weeks and bleaching alert level 2 (NOAA, 2021) with no signs of bleaching in the reef (Israel National Monitoring Program of the Gulf of Eilat, 2021).

3.2 Monthly in-situ assessment of coral and symbiont physiology before and after a marine heatwave

3.2.1 Algal density and chlorophyll content

Algal density of *S. pistillata and P. damicornis* (Figures 2A, C, respectively) remained similar across the MHW (pre, during, and post MHW; July-September) but overall had higher symbiont densities in winter (December, January-February) than summer (June-September; Table 3). *Stylophora* harbored on average 2-fold more symbionts per surface area than *Pocillopora*. Variation in symbiont densities among parent colonies in *Stylophora* was higher than that of *Pocillopora* (Table 3).

Chlorophyll-a concentrations (Figures 2B, D) in symbionts of both species did not vary significantly across the MHW (Table 3), but were lower during the MHW than the annual average by 4% (*Stylophora*), and by 2% in *P. damicornis* (Tables 1, 2). Variation in chlorophyll concentration among parent colonies in *Pocillopora* was higher than that of *Stylophora* (Table 3).

3.2.2 Pulse amplitude modulated fluorometry

Significantly higher maximum quantum yields of photosystem II (F_v/F_m) in *S. pistillata* (+6%; Figure 3A) and *P. damicornis* (+12%; Figure 3E) were detected during May-January, encompassing the MHW, compared to late winter-spring (February-April), before the MHW. Rapid light curves (Supplementary Figure S2; Table 3) indicated that the maximal relative electron transport rates ($rETR_{max}$; Figure 3B) in *S. pistillata* were 45% higher following the MHW (September-November) than before it began (July), and significantly higher than all other months. $rETR_{max}$ in *P. damicornis* (Figure 3F) did not vary across the MHW but were overall higher (+40%) in late summer-fall (including the MHW period), compared

TABLE 2 Seasonal variation (averaged maximum and minimum values, excluding August), and averaged values during the MHW (August) ± STD in *Pocillopora damicornis*.

	Seasonal range	MHW average
Algal density (Cells cm^{-2})	2.5*10^6 ± 7.6*10^5 (Jan)-1.5*10^6 ± 7.2*10^5 (Jun)	1.8*10^6± 4.6*10^5
Chlorophyll (pg cell^{-1})	1.7 ± 0.66 (Feb)-0.88 ± 0.29 (Oct)	1.2 ± 0.2
Fv/Fm	0.62 ± 0.02 (Oct)-0.54 ± 0.03 (Apr)	0.59 ± 0.03
rETRmax	37.27 ± 10.09 (Nov)-13.69 ± 3.78 (Jan)	35.09 ± 7.68
iK	8.43 ± 1.35 (Nov)-3.22 ± 0.82 (Jan)	7.07 ± 1.19
Alpha	5.28 ± 0.36 (Oct)-4.10 ± 0.34 (Feb)	4.93 ± 0.41
Host proteins (mg cm^{-2})	1.15 ± 0.6 (May)-0.52 ± 0.08 (Nov)	0.89 ± 0.24
Host carbohydrates (mg cm^{-2})	0.17 ± 0.07 (May)-0.09 ± 0.04 (Nov)	0.10 ± 0.03
Host lipids (mg cm^{-2})	0.40 ± 0.25 (Mar)-0.18 ± 0.13 (Jun)	0.39 ± 0.22
Host total energy (J cm^{-2})	46.25 ± 25.57 (May)-25.88 ± 8.1 (Nov)	40.71 ± 8.08
Symbiont proteins (pg cell^{-1})	47.54 ± 15.01 (May)-29.68 ± 15.73 (Jan)	40.03 ± 10.01
Symbiont carbohydrates (pg cell^{-1})	45.66 ± 15.72 (Mar)-23.48 ± 3.6 (Jan)	24.08 ± 4.20
Symbiont lipids (pg cell^{-1})	42.52 ± 29 (Dec)-18.82 ± 16.64 (Sep)	28.03 ± 16.89
Symbiont total energy (µJ cell^{-1})	3.69 ± 1.6 (Dec)-1.84 ± 0.91 (Jan)	2.52 ± 0.87

with winter-spring, before the MHW. *Stylophora* and *Pocillopora* presented higher (24 and 37%, respectively) rETRmax values than the annual average during August (Tables 1, 2).

Following the MHW, the iK values (Figure 3C) in September were highest for *S. pistillata*, and 47 and 36% higher than in July and August, respectively. The photosynthetic efficiency under low irradiances, alpha (Figure 3D), was the highest across months at the onset of the MHW and significantly higher compared to July (14%) and September (12%; Table 3). Alpha values in *Stylophora* symbionts during August were substantially higher compared to values in winter (December, January, February), spring (March-May), and early summer (June).

The iK values of the symbionts of *P. damicornis* (Figure 3G) did not vary during the MHW. However, higher iK values were seen during summer-fall (July-November) relative to winter-spring. Alpha values of the *P. damicornis* symbionts (Figure 3H) were 11 and 13% higher in July and August, respectively, compared to September.

Taken together, all photosynthetic parameters in symbionts of both species were higher during the MHW compared with the annual average (Tables 1, 2).

3.2.3 Proteins, carbohydrates, lipids, and total energy

The two examined species demonstrated distinct responses to the MHW.

S. pistillata

During the MHW (August), the only, but significant catabolic response was a decline of 33% in host proteins (storage and structural) compared to July, before the MHW (Figure 4A; Table 3), and 24% lower than the annual average (Table 1). Recovery of host protein levels was recorded by January. Symbionts, however, had more proteins (12%) during the MHW relative to the annual average (Figure 4E). The parent colony identity may explain 26% of the variability of host proteins and 15% of the symbiont protein content.

Host carbohydrates did not differ before and after the MHW, yet fewer carbohydrates were detected during summer months relative to the annual average (Figure 4B; Table 1), and significantly lower (50%) than in April, when carbohydrates were highest (Table 3). The symbiont carbohydrates increased by 33% from the onset (August) to the end of the MHW (September), with the lowest content measured in August and the highest in spring (Figure 4F). 22% of the variability in host carbohydrates, and 46% of the symbiont carbohydrates, may be explained by the parent-colony identity.

Host lipids were similar before, during, and after the MHW, with the lowest values seen during August (Figure 4C). Host lipids during the MHW were lower (40%) than the annual average (Table 1). In contrast, symbiont lipids increased by 41% compared to their seasonal average (Figure 4G; Table 1).

The total energy of the host was lowest at the onset of the MHW (Figure 4D), substantially lower than in late spring and early winter, and lower (34%) than the annual average (Table 1). In contrast, symbionts' total energy presented the highest values across summer

TABLE 3 Statistical analyses of differences in physiological parameters between months by species.

	Stylophora pistillata		*Pocillopora damicornis*	
rETRmax	m: 6.49	F: 30.7	m: 21.29	F: 19.33
	c: 28.91	**p<0.0001**	c: 30.94	**p<0.0001**
Fv/Fm	m: 0.0002	F: 11.169	m: 0.0001	F: 51.093
	c: 0.0003	**p<0.0001**	c: 0.0003	**p<0.0001**
Alpha	m: 0.01	F: 15.61	m: 0.030	F: 18.77
	c: 0.07	**p<0.0001**	c: 0.068	**p<0.0001**
iK	m: 0.08	F: 63.9	m: 0.60	F: 15.34
	c: 0.57	**p<0.0001**	c: 1.22	**p<0.0001**
Algal density (cells cm^{-2})	m: $2.172*10^{11}$	F: 20.83	m: $8.36*10^{10}$	F: 4.075
	c: $4.325*10^{11}$	**p<0.0001**	c: $2.488*10^{11}$	**p<0.0001**
Chlorophyll (chl $cell^{-1}$)	m: $8.136*10^{-5}$	F: 5.743	m: 0.005	F: 6.845
	c: $5.002*10^{-2}$	**p<0.0001**	c: 0.081	**p<0.0001**
Host Proteins (mg cm^{-2})	m: 0.0162	F: 6.763	m: 0.006	F: 7.005
	c: 0.046	**p< 0.0001**	c: 0.024	**p<0.0001**
Symbiont proteins (pg $cell^{-1}$)	m: 11.75	F: 8.481	m: 18.78	F: 1.780
	c: 66.52	**p<0.0001**	c: 126.56	p>0.05
Host carbohydrates (mg cm^{-2})	m: 0.0008	F: 6.2686	m: 0.0001	F: 5.653
	c: 0.0028	**p<0.0001**	c: 0.0011	**p< 0.0001**
Symbiont carbohydrates (pg $cell^{-1}$)	m: 0.00024	F: 22.716	m: 0.00005	F: 13.508
	c: 0.00028	**p<0.0001**	c: 0.0002	**p<0.0001**
Host lipids (mg cm^{-2})	m: 0.0005	F: 3.852	m: 0.000	F: 2.0473
	c: 0.0432	**p<0.0001**	c: 0.035	**p<0.032**
Symbiont lipids (pg $cell^{-1}$)	m: †	F: 2.4022	m: †	F: 0.90924
	c:	**p< 0.024**	c:	p>0.05
Host total energy (J cm^{-2})	m: 22.5	F: 4.9651	m: †	F: 3.268
	c: 106.2	**p<0.0001**	c:	**p<0.003**
Symbiont total energy (µJ $cell^{-1}$)	m: 0.000	F: 5.527	m: 0.08368	F: 0.9556
	c: 0.2521	**p<0.0001**	c: 0.86250	p>0.05

Outcomes were obtained from linear mixed models (LMM), with months defined as the fixed factor, while parent-colony was defined as the random factor. Linear mixed models were performed if residuals were distributed normally with equal variances. If the LMM assumptions were not met, PERMANOVA was conducted, as indicated by †. P-values in bold indicate a significant difference (α=0.05)."m" (marginal R^2 values) is the proportion of variance explained by the fixed factors only (month), while "c" (conditional R^2 values) is the proportion of variance described by random and fixed factors (parent-colony and month).

(Figure 4H), with higher values (9%) than the seasonal average (Table 1).

P. damicornis

Host proteins (storage and structural) did not alter significantly during the MHW (Figure 5A) yet were higher (7%) than the annual average (Table 2). The total proteins of symbionts did not differ significantly across seasons and through the MHW (Figure 5E). However, symbiont protein declined by 7% relative to the seasonal average during the MHW (Table 2). The parent-colony identity may explain 20% of the overall variability in host proteins and 13% in symbiont proteins (Table 3).

Host carbohydrates did not vary before and after the MHW, with the highest content measured in April-May (Figure 5B). Similarly, symbiont carbohydrates remained similar across the MHW, yet values at the onset of the MHW were considerably lower compared to values in spring (Figure 5F). Both host and symbiont carbohydrates declined during the MHW by 21 and 46%, respectively, than their annual average (Table 2). The parent colony identity may explain 8% of the overall variability of host carbohydrates and 20% of the symbiont carbohydrates (Table 3).

Host and symbiont lipids did not vary considerably throughout the MHW nor across months (Figures 5C, G, respectively). However, host

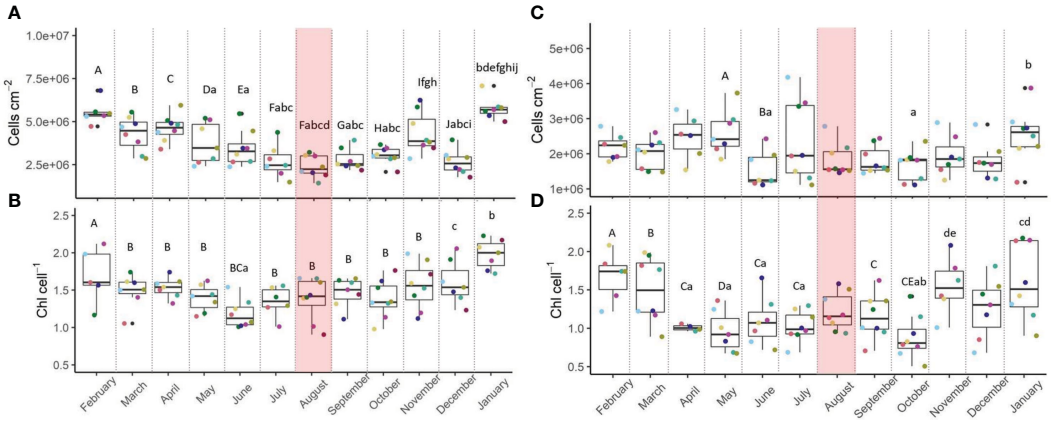

FIGURE 2
Algal density and chlorophyll concentration of *Stylophora pistillata* **(A, B)** and in *Pocillopora damicornis* **(C, D)**, from February 2021 to January 2022. n=8. Shaded red area denotes the marine heatwave. Boxes display the median line, the first and third quartiles (box outline) and whiskers are 1.5 times the interquartile range. Colored points denote coral parent-colony, consistent to all plots. Black points are outliers. Letters of upper and lower cases denote significant differences between months (Linear Mixed Effect Model and Tukey *post-hoc* test).

lipids increased during the MHW by 24%, and symbiont lipids decreased by 2%, than their annual average (Table 2).

The total energy of *P. damicornis* host and symbionts (Figures 5D, H) did not differ before and after the MHW. However, substantially higher total energy of the host was recorded in August and spring compared to fall months (October and November). Total energy during the MHW in host and symbionts was higher (20%) and lower (11%), respectively, than their annual average (Table 2).

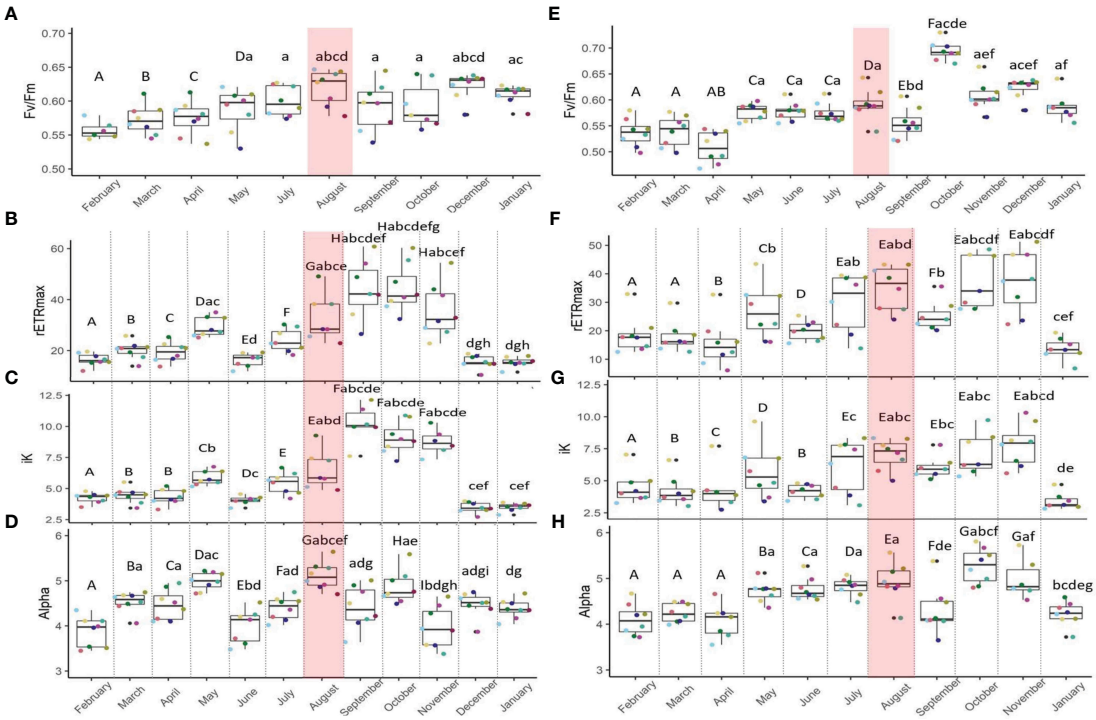

FIGURE 3
Maximal quantum yield (Fv/Fm; **A**, **E**), maximal rETR (rETRmax; **B**, **F**), iK **(C, G)** and alpha **(D, H)** of *Stylophora pistillata* and *Pocillopora damicornis* symbionts, respectively, from February 2021 to January 2022. n=8. The shaded red area denotes the marine heatwave. Boxes display the median line, the first and third quartiles (box outline) and whiskers are 1.5 times the interquartile range. Colored points denote coral parent-colony, consistent to all plots. Black point are outliers. Letters of upper and lower cases denote significant differences between months (Linear Mixed Effect Model and Tukey *post hoc* test).

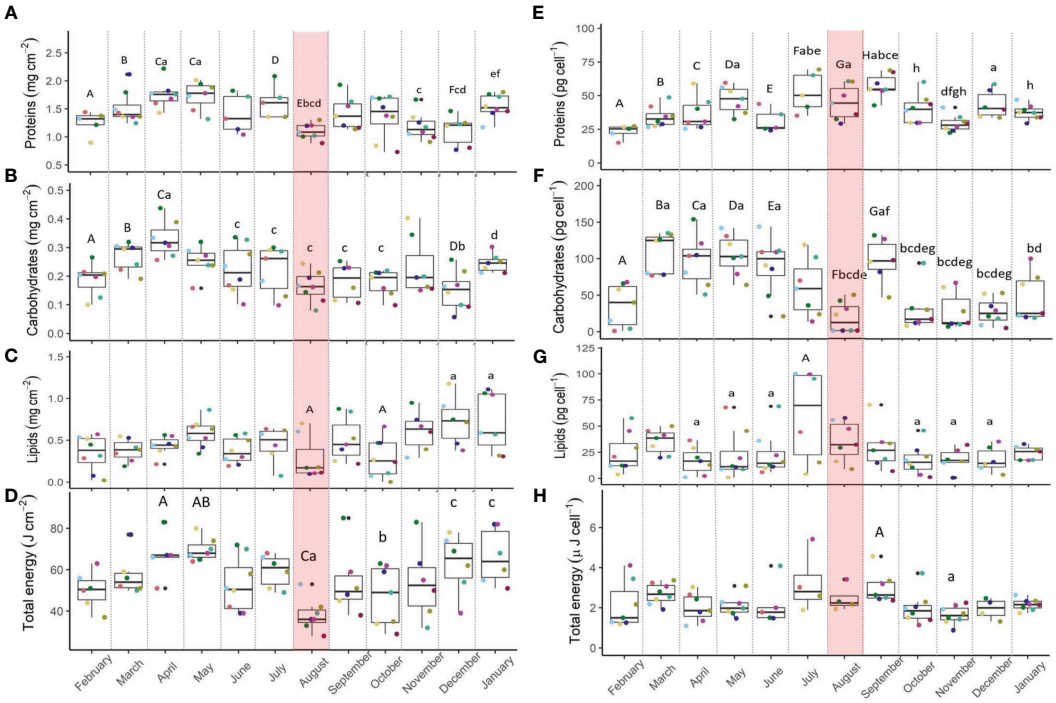

FIGURE 4
Stylophora pistillata host proteins **(A)**, carbohydrates **(B)**, lipids **(C)** and total energy reserves **(D)** and symbiont proteins **(E)**, carbohydrates **(F)**, lipids **(G)** and stored energy reserves **(H)**, from February 2021 to January 2022. n=8. Shaded red area denotes the marine heatwave. Boxes display the median line, the first and third quartiles (box outline) and whiskers are 1.5 times the interquartile range. Colored points denote coral parent-colony, consistent to all plots. Black points are outliers. Letters of upper and lower cases denote significant differences between months (Linear Mixed Effect Model and Tukey *post hoc* test or PERMANOVA).

4 Discussion

In this study, we examined the response of common GoA corals, a potential coral refuge from climate change, to a naturally occurring MHW. The results highlight the remarkable resilience of GoA corals to MHWs with no mortality, bleaching, photosynthetic deficiency, and lethal catabolic effects. These results are different from the outcomes of MHWs reported from coral reefs in the Great Barrier Reef (Leggat et al., 2019; Brown et al., 2023), Andaman Sea (Krishnan et al., 2011), Western Australia (Depczynski et al., 2013), and Seychelles (Spencer et al., 2000), all resulting in mass coral bleaching and mortality (reviewed in Shlesinger and van Woesik, 2023).

A monthly *in-situ* physiological baseline for these species on this site is lacking. However, *Pocillopora verrucossa* sampled along a 12° latitudinal gradient, ranging from the GoA to the Farasan Islands in the southern Red Sea, had consistent protein values in summer (September) than in winter (March; Sawall et al., 2015), similar to *P. damicornis* in this study during the same months. However, *P. verrucossa* exhibited higher lipid content in summer (Sawall et al., 2015), whereas here *P. damicornis* had similar lipid values.

Species-specific physiological plasticity is the ability of different species to adjust their physiology in response to changing environmental conditions (Ziegler et al., 2014; Hoadley et al., 2015). During periods of food scarcity, such as under thermal stress when photosynthates are retained by the symbionts (Rädecker et al., 2021; Allen-Waller and Katie, 2023), corals reduce their metabolism to conserve energy (Innis et al., 2021), and some increase heterotrophy (Grottoli et al., 2006). Species that fail to sustain their energetic needs may perish, leading to rapid shifts in coral community composition or phase shifts to algal dominance (Loya et al., 2001; Fordyce et al., 2019).

In this study, the only significant change in coral physiology during the MHW was in *Stylophora pistillata*, which had significantly reduced protein levels compared to July, before the MHW. Proteins, the most functional macromolecule group, are crucial in repairing and stabilizing physiological processes impacted by elevated temperatures in corals (Gates and Edmunds, 1999). Proteins vary in abundance during thermal stress based on their function (Petrou et al., 2021); Calcium-binding, antioxidants, and heat shock proteins (HSPs) are induced during cellular damage and stress responses in corals (HSPs; Barshis et al., 2013; Petrou et al., 2021; Savary et al., 2021). However, their abundance can also be temporal, as HSP70, a well-known HSP in corals, may present varying levels under constant thermal stress, suggesting that rapid protein turnover provides flexibility and acclimatization potential (Gates and Edmunds, 1999). In addition, *Stylophora* significantly decreased feeding rates at 31°C (Ferrier-Pagès et al., 2010), potentially leading to scarcity of building blocks for protein synthesis. A study on RNA expression, the precursor to protein synthesis, revealed that *S. pistillata* from the GoA rapidly elevated its gene expression while demonstrating transcriptional resilience and recovery abilities up to 32°C (Savary et al., 2021). A high-resolution proteomic research approach could serve as a fruitful research field in GoA corals to better understand the functions of the coral host proteins under thermal stress and oxidative damage.

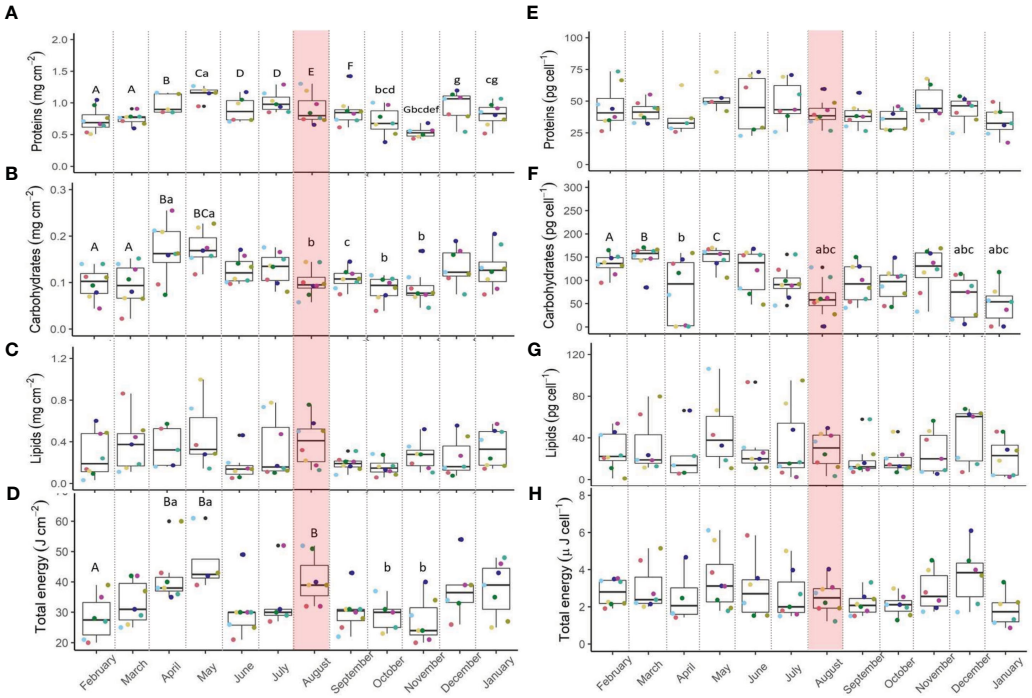

FIGURE 5
Pocillopora damicornis host proteins **(A)**, carbohydrates **(B)**, lipids **(C)** and total energy reserves **(D)** and symbiont proteins **(E)**, carbohydrates **(F)**, lipids **(G)** and stored energy reserves **(H)**, from February 2021 to January 2022. n=8. Shaded red area denotes the marine heatwave. Boxes display the median line, the first and third quartiles (box outline) and whiskers are 1.5 times the interquartile range. Colored points denote coral parent-colony, consistent to all plots. Black points are outliers. Letters of upper and lower cases denote significant differences between months (Linear Mixed Effect Model and Tukey *post hoc* test or PERMANOVA).

Although *Pocillopora* had considerably lower energy reserves baseline levels (proteins:-41%, carbohydrates:-45%, lipids:-34%) than *Stylophora* and harbored the relatively sensitive *Cladocopium* symbiont (Karako-Lampert et al., 2004), it maintained its energy reserves during the MHW. Therefore, *P. damicornis* may be more thermally-resilient than *S. pistillata* (this study; Sebastián et al., 2009; Grottoli et al., 2017).

The physiological responses of the two holobionts in the present study were to a category II (strong) MHW, with a maximal intensity (I_{max}) of 3.5˚C and an onset rate (R_{onset}) of 0.3 (Hobday et al., 2016; Hobday et al., 2018). While an onset rate of +1˚C/day was found to affect bleaching severity under simulated MHW in corals of Western Australia (Sahin et al., 2023), in studies conducted in the GoA, the temperature was often ramped by +1˚C/day without

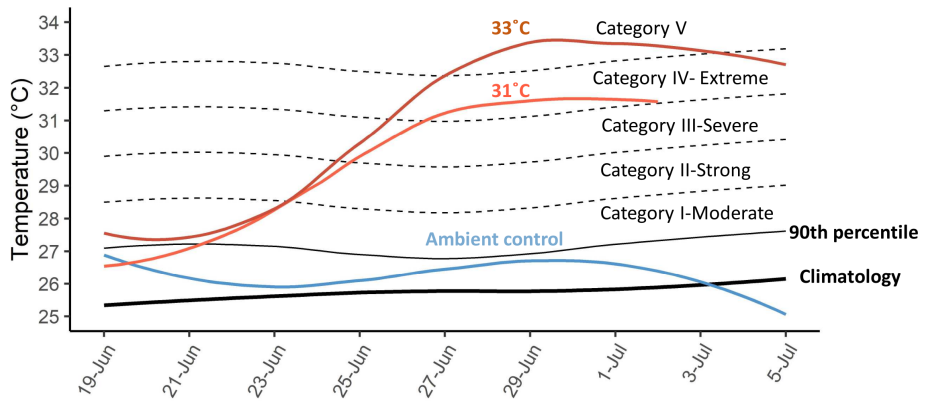

FIGURE 6
Simulated marine heatwaves (data taken from Kochman et al., 2021) categories after Hobday et al. (2018). Black lines represent the 31-year regional climatology (thick line; Israel National Monitoring Program of the Gulf of Eilat, 2017), the 90th percentile climatology (thin line), and multiples (X2, X3, X4, X5) of the delta between the 90th percentile and the long-term climatology during the dates of the experiment. The temperature treatments are depicted for ambient control (blue), the 31˚C (light orange), and 33˚C (dark orange) treatments.

inducing signs of physiological stress (Bellworthy and Fine, 2017; Kochman et al., 2021).

S. pistillata from the northern GoA can survive a simulated category IV (extreme) MHW (31˚C; I_{max}=5.9, R_{onset}=1˚C/day; Figure 6; Kochman et al., 2021). Survival was genotype-specific when inflicted with a category V MHW (33˚C; I_{max}=7.8, R_{onset}=1˚C/day). The capacity of *S. pistillata* to endure the hottest MHW *in-situ* and a simulated, more intense MHW emphasize the high temperatures this species can withstand in the GoA (up to 33° C; Voolstra et al., 2021). Nonetheless, the remarkable resistance of GoA corals to future ocean conditions may be jeopardized by local pollutants (Hall et al., 2018; Banc-Prandi and Fine, 2019; Fine et al., 2019), yet mitigating local stressors may assist in coral recovery following MHWs (Donovan et al., 2021).

As the occurrence of MHWs raised by 2-fold in the last decade (Oliver et al., 2018) and half of the oceans are projected to reside in a permanent MHW by the end of the century (Oliver et al., 2019), it is of great interest to better understand the species-specific plasticity and resilience mechanisms of GoA corals, a potential coral refuge (Osman et al., 2018). MHWs were not recorded in the GoA in the last decades until 2015 (Genevier et al., 2019), and there are no studies predicting their intensity and frequency in the near future. More research is needed to identify how multiple coral species in a potential coral refuge respond to different intensities, frequencies, and onset rates of both ambient and simulated MHWs. Finally, this unique coral refuge may serve as a source of propagules in more southern, damaged reefs in the Red Sea (Fine et al., 2019).

Data availability statement

The original contributions presented in the study are publicly available. This data can be found here: https://github.com/Coral-NRG/Marine_heatwave_2021_GoA.

Ethics statement

The animal study was approved by Israeli National Park Authority. The study was conducted in accordance with the local legislation and institutional requirements.

Author contributions

N-RK-G and MF conceived, designed, performed the experiment, analyzed the data, and wrote the paper. All authors contributed to the article and approved the submitted version.

Funding

This research was funded by the Red Sea Reef Foundation (grant no. (2020638 granted to N-RK-G, and partially supported by a US AID grant (MERC M38-013) to MF.

Acknowledgments

The authors would like to convey their deepest gratitude to Chen Azulay, Dror Komet, Britt Ronen, and Daniel Gino for their valuable assistance during sampling and tissue processing. The authors thank Prof. Amatzia Genin for providing additional temperature data.

Conflict of interest

The authors declare that the research was conducted in the absence of any commercial or financial relationships that could be construed as a potential conflict of interest.

Publisher's note

Supplementary material

The Supplementary Material for this article can be found online at: https://www.frontiersin.org/articles/10.3389/fmars.2023.1215567/full#supplementary-material

SUPPLEMENTARY FIGURE 1
Maximal daily temperature during the marine heatwave (purple), the 33-year climatology (bolded black), the 90th percentile climatology (thin black), and the difference between the 90th temperature percentile and mean climatology value (dashed line), after Hobday et al. (2018).

SUPPLEMENTARY FIGURE 2
Averaged relative electron transport rate (rETR) of *Stylophora pistillata* **(A)** *and Pocillopora damicornis* **(B)** symbionts to increasing light intensity (0 to 701 µmol photons m^{-2} s^{-1}) from February 2021 to January 2022. n=8.

References

Alamaru, A., Loya, Y., Brokovich, E., Yam, R., and Shemesh, A. (2009). Carbon and nitrogen utilization in two species of Red Sea corals along a depth gradient: Insights from stable isotope analysis of total organic material and lipids. *Geochim. Cosmochim. Acta* 73, 5333–5342. doi: 10.1016/j.gca.2009.06.018

Allen-Waller, L., and Katie, W. (2023). Symbiotic dinoflagellates divert energy away from mutualism during coral bleaching recovery. *Symbiosis* 89 (2), 173–186. doi: 10.1007/s13199-023-00901-3

Baird, A. H., and Marshall, P. A. (2002). Mortality, growth and reproduction in scleractinian corals following bleaching on the Great Barrier Reef. *Mar. Ecol. Prog. Ser.* 237, 133–141. doi: 10.3354/meps237133

Banc-Prandi, G., and Fine, M. (2019). Copper enrichment reduces thermal tolerance of the highly resistant Red Sea coral Stylophora pistillata. *Coral Reefs* 38, 285–296. doi: 10.1007/s00338-019-01774-z

Barshis, D. J., Ladner, J. T., Oliver, T. A., Seneca, F. O., Traylor-Knowles, N., and Palumbi, S. R. (2013). Genomic basis for coral resilience to climate change. *Proc. Natl. Acad. Sci. USA* 110, 1387–1392. doi: 10.1073/pnas.1210224110

Barton, K. (2020). *MuMIn: Multi-model inference. R package version 1.43. 17. 2020.* Available at: https://cran.r-project.org/package=MuMIn.

Bates, D., Mächler, M., Bolker, B., and Walker, S. (2014). Fitting linear mixed-effects models using lme4. *arXiv preprint arXiv:1406.5823*.

Bellworthy, J., and Fine, M. (2017). Beyond peak summer temperatures, branching corals in the Gulf of Aqaba are resilient to thermal stress but sensitive to high light. *Coral Reefs* 36, 1071–1082. doi: 10.1007/s00338-017-1598-1

Brown, K. T., Eyal, G., Dove, S. G., and Barott, K. L. (2023). Fine-scale heterogeneity reveals disproportionate thermal stress and coral mortality in thermally variable reef habitats during a marine heatwave. *Coral Reefs* 42 (1), 131–142. doi: 10.1007/s00338-022-02328-6

Byler, K. A., Carmi-Veal, M., Fine, M., and Goulet, T. L. (2013). Multiple symbiont acquisition strategies as an adaptive mechanism in the coral Stylophora pistillata. *PloS One* 8, 1–7. doi: 10.1371/journal.pone.0059596

Cantin, N. E., and Lough, J. M. (2014). Surviving coral bleaching events: Porites growth anomalies on the Great Barrier Reef. *PloS One* 9, e88720. doi: 10.1371/journal.pone.0088720

Cheng, Y. S., Zheng, Y., and VanderGheynst, J. S. (2011). Rapid quantitative analysis of lipids using a colorimetric method in a microplate format. *Lipids* 46, 95–103. doi: 10.1007/s11745-010-3494-0

Depczynski, M., Gilmour, J. P., Ridgway, T., Barnes, H., Heyward, A. J., Holmes, T. H., et al. (2013). Bleaching, coral mortality and subsequent survivorship on a West Australian fringing reef. *Coral Reefs* 32, 233–238. doi: 10.1007/s00338-012-0974-0

Dobson, K. L., Ferrier-Pagès, C., Saup, C. M., and Grottoli, A. G. (2021). The effects of temperature, light, and feeding on the physiology of pocillopora damicornis, stylophora pistillata, and turbinaria reniformis corals. *Water (Switzerland)* 13 (15), 2048. doi: 10.3390/w13152048

Donovan, M. K., Burkepile, D. E., Kratochwill, C., Shlesinger, T., Sully, S., Oliver, T. A., et al. (2021). Local conditions magnify coral loss after marine heatwaves. *Sci. (80-.).* 372, 977–980. doi: 10.1126/science.abd9464

Eddy, T. D., Lam, V. W. Y., Reygondeau, G., Cisneros-Montemayor, A. M., Greer, K., Palomares, M. L. D., et al. (2021). Global decline in capacity of coral reefs to provide ecosystem services. *One Earth* 4, 1278–1285. doi: 10.1016/j.oneear.2021.08.016

Evensen, N. R., Fine, M., Perna, G., Voolstra, C. R., and Barshis, D. J. (2021). Remarkably high and consistent tolerance of a Red Sea coral to acute and chronic thermal stress exposures. *Limnol. Oceanogr.* 66 (5), 1718–1729. doi: 10.1002/lno.11715

Ferrier-Pagès, C., Rottier, C., Beraud, E., and Levy, O. (2010). Experimental assessment of the feeding effort of three scleractinian coral species during a thermal stress: Effect on the rates of photosynthesis. *J. Exp. Mar. Bio. Ecol.* 390, 118–124. doi: 10.1016/j.jembe.2010.05.007

Fine, M., Cinar, M., Voolstra, C. R., Safa, A., Rinkevich, B., Laffoley, D., et al. (2019). Coral reefs of the Red Sea — Challenges and potential solutions. *Reg. Stud. Mar. Sci.* 25, 1–13. doi: 10.1016/j.rsma.2018.100498

Fine, M., Gildor, H., and Genin, A. (2013). A coral reef refuge in the Red Sea. *Glob. Change Biol.* 19, 3640–3647. doi: 10.1111/gcb.12356

Fordyce, A. J., Ainsworth, T. D., Heron, S. F., and Leggat, W. (2019). Marine heatwave hotspots in coral reef environments: Physical drivers, ecophysiological outcomes and impact upon structural complexity. *Front. Mar. Sci.* 6. doi: 10.3389/fmars.2019.00498

Frölicher, T. L., Fischer, E. M., and Gruber, N. (2018). Marine heatwaves under global warming. *Nature* 560, 360–364. doi: 10.1038/s41586-018-0383-9

Gates, R. D., and Edmunds, P. J. (1999). The physiological mechanisms of acclimatization in tropical reef corals. *Am. Zool.* 39, 30–43. doi: 10.1093/icb/39.1.30

Genevier, L. G. C., Jamil, T., Raitsos, D. E., Krokos, G., and Hoteit, I. (2019). Marine heatwaves reveal coral reef zones susceptible to bleaching in the Red Sea. *Glob. Change Biol.* 25, 2338–2351. doi: 10.1111/gcb.14652

Genin, A., Levy, L., Sharon, G., Raitsos, D. E., and Diamant, A. (2020). Rapid onsets of warming events trigger mass mortality of coral reef fish. *Proc. Natl. Acad. Sci. USA* 117, 25378–25385. doi: 10.1073/pnas.2009748117

Gnaiger, E., and Bitterlich, G. (1984). Proximate biochemical composition and caloric content calculated from elemental CHN analysis: a stoichiometric concept. *Oecologia* 62, 289–298. doi: 10.1007/BF00384259

Grottoli, A. G., Rodrigues, L. J., and Juarez, C. (2004). Lipids and stable carbon isotopes in two species of Hawaiian corals, Porites compressa and Montipora verrucosa, following a bleaching event. *Mar. Biol.* 145, 621–631. doi: 10.1007/s00227-004-1337-3

Grottoli, A. G., Rodrigues, L. J., and Palardy, J. E. (2006). Heterotrophic plasticity and resilience in bleached corals. *Nature* 440, 1186–1189. doi: 10.1038/nature04565

Grottoli, A. G., Tchernov, D., and Winters, G. (2017). Physiological and biogeochemical responses of super-corals to thermal stress from the northern gulf of Aqaba, Red Sea. *Front. Mar. Sci.* 4. doi: 10.3389/fmars.2017.00215

Hall, E. R., Muller, E. M., Goulet, T., Bellworthy, J., Ritchie, K. B., and Fine, M. (2018). Eutrophication may compromise the resilience of the Red Sea coral Stylophora pistillata to global change. *Mar. pollut. Bull.* 131, 701–711. doi: 10.1016/j.marpolbul.2018.04.067

Hoadley, K. D., Pettay, D. T., Grottoli, A. G., Cai, W. J., Melman, T. F., Schoepf, V., et al. (2015). Physiological response to elevated temperature and pCO2 varies across four Pacific coral species: Understanding the unique host+symbiont response. *Sci. Rep.* 5, 1–15. doi: 10.1038/srep18371

Hobday, A. J., Alexander, L. V., Perkins, S. E., Smale, D. A., Straub, S. C., Oliver, E. C. J., et al. (2016). A hierarchical approach to defining marine heatwaves. *Prog. Oceanogr.* 141, 227–238. doi: 10.1016/j.pocean.2015.12.014

Hobday, A. J., Oliver, E. C. J., Gupta, A., Benthuysen, J. A., Burrows, M. T., Donat, M. G., et al. (2018). Categorizing and naming marine heatwaves. *Oceanography* 31, 162–173. doi: 10.5670/oceanog.2018.205

Hoegh-Guldberg, O. (1999). Climate change, coral bleaching and the future of the world's coral reefs. *Mar. Freshw. Res.* 50, 839–866. doi: 10.1071/MF99078

Hoegh-Guldberg, O. (2011). Coral reef ecosystems and anthropogenic climate change. *Reg. Environ. Change* 11, 215–227. doi: 10.1007/s10113-010-0189-2

Hoegh-Guldberg, O., and Jones, R. J. (1999). Photoinhibition and photoprotection in symbiotic dinoflagellates from reef-building corals. *Mar. Ecol. Prog. Ser.* 183, 73–86. doi: 10.3354/meps183073

Hoegh-Guldberg, O., Mumby, P. J., Hooten, A. J., Steneck, R. S., Greenfield, P., Gomez, E., et al. (2007). Coral reefs under rapid climate change and ocean acidification. *Science* 318, 1737–1742. doi: 10.1126/science.1152509

Hughes, T. P., Anderson, K. D., Connolly, S. R., Heron, S. F., Kerry, J. T., Lough, J. M., et al. (2018). Spatial and temporal patterns of mass bleaching of corals in the Anthropocene. *Sci. (80-.).* 359, 80–83. doi: 10.1126/science.aan8048

Hughes, T. P., Kerry, J. T., Álvarez-Noriega, M., Álvarez-Romero, J. G., Anderson, K. D., Baird, A. H., et al. (2017). Global warming and recurrent mass bleaching of corals. *Nature* 543, 373–377. doi: 10.1038/nature21707

Imbs, A. B., and Yakovleva, I. M. (2012). Dynamics of lipid and fatty acid composition of shallow-water corals under thermal stress: an experimental approach. *Coral Reefs* 31, 41–53. doi: 10.1007/s00338-011-0817-4

Innis, T., Allen-Waller, L., Brown, K. T., Sparagon, W., Carlson, C., Kruse, E., et al. (2021). Marine heatwaves depress metabolic activity and impair cellular acid–base homeostasis in reef-building corals regardless of bleaching susceptibility. *Glob. Change Biol.* 27, 2728–2743. doi: 10.1111/gcb.15622

Israel National Monitoring Program of the Gulf of Eilat (2017). *Annual report 2017.* Available at: https://iui-eilat.huji.ac.il/uploaded/NMP/reports/NMPReport2017.pdf.

Israel National Monitoring Program of the Gulf of Eilat (2021). *Israel National Monitoring Program of the Gulf of Eilat.* Available at: http://www.meteo-tech.co.il/eilat-yam/eilat_about_en.asp (Accessed January 11, 2022).

Israel National Monitoring Program of the Gulf of Eilat (2022). *Israel National Monitoring Program of the Gulf of Eilat.* Available at: http://www.meteo-tech.co.il/eilat-yam/eilat_about_en.asp (Accessed January 11, 2022).

Jeffrey, S. W. T., and Humphrey, G. F. (1975). New spectrophotometric equations for determining chlorophylls a, b, c1 and c2 in higher plants, algae and natural phytoplankton. *Biochem. und Physiol. der Pflanz.* 167, 191–194. doi: 10.1016/S0015-3796(17)30778-3

Jones, R. J., Hoegh-Guldberg, O., Larkum, A. W. D., and Schreiber, U. (1998). Temperature-induced bleaching of corals begins with impairment of the CO2 fixation mechanism in zooxanthellae. *Plant Cell Environ.* 21, 1219–1230. doi: 10.1046/j.1365-3040.1998.00345.x

Karako-Lampert, S., Katcoff, D. J., Achituv, Y., Dubinsky, Z., and Stambler, N. (2004). Do clades of symbiotic dinoflagellates in scleractinian corals of the Gulf of Eilat (Red Sea) differ from those of other coral reefs? *J. Exp. Mar. Bio. Ecol.* 311, 301–314. doi: 10.1016/j.jembe.2004.05.015

Kleinhaus, K., Al-Sawalmih, A., Barshis, D. J., Genin, A., Grace, L. N., Hoegh-Guldberg, O., et al. (2020). Science, diplomacy, and the red sea's unique coral reef: it's time for action. *Front. Mar. Sci.* 7. doi: 10.3389/fmars.2020.00090

Kochman, N. R., Grover, R., Rottier, C., Ferrier-Pages, C., and Fine, M. (2021). The reef building coral Stylophora pistillata uses stored carbohydrates to maintain ATP levels under thermal stress. *Coral Reefs* 40, 1473–1485. doi: 10.1007/s00338-021-02174-y

Krishnan, P., Roy, S. D., George, G., Srivastava, R. C., Anand, A., Murugesan, S., et al. (2011). Elevated sea surface temperature during May 2010 induces mass bleaching of corals in the Andaman. *Curr. Sci.*, 111–117.

Krueger, T., Horwitz, N., Bodin, J., Giovani, M. E., Escrig, S., Meibom, A., et al. (2017). Common reef-building coral in the northern red sea resistant to elevated temperature and acidification. *R. Soc Open Sci.* 4 (5), 170038. doi: 10.1098/rsos.170038

Lampert-Karako, S., Stambler, N., Katcoff, D. J., Achituv, Y., Dubinsky, Z., and Simon-Blecher, N. (2008). Effects of depth and eutrophication on the zooxanthella clades of Stylophora pistillata from the Gulf of Eilat (Red Sea). *Aquat. Conserv. Mar. Freshw. Ecosyst.* 18, 1039–1045. doi: 10.1002/aqc.927

Leggat, W. P., Camp, E. F., Suggett, D. J., Heron, S. F., Fordyce, A. J., Gardner, S., et al. (2019). Rapid coral decay is associated with marine heatwave mortality events on reefs. *Curr. Biol.* 29, 2723–2730.e4. doi: 10.1016/j.cub.2019.06.077

Lenth, R., Singmann, H., Love, J., Buerkner, P., and Herve, M. (2018). Estimated marginal means, aka Least-Squares Means. *R package version 1.2*. Available at: https://Https://CRAN. R-Project. Org/Package= emmeans.

Loya, Y., Sakai, K., Yamazato, K., Nakano, Y., Sambali, H., and Van Woesik, R. (2001). Coral bleaching: the winners and the losers. *Ecol. Lett.* 4, 122–131. doi: 10.1046/j.1461-0248.2001.00203.x

Masuko, T., Minami, A., Iwasaki, N., Majima, T., Nishimura, S. I., and Lee, Y. C. (2005). Carbohydrate analysis by a phenol-sulfuric acid method in microplate format. *Anal. Biochem.* 339, 69–72. doi: 10.1016/j.ab.2004.12.001

NOAA (2021). *NOAA Coral Reef Watch Homepage and Near-Real-Time Products Portal*. Available at: https://coralreefwatch.noaa.gov/satellite/index.php (Accessed December 28, 2020).

Oksanen, J. (2007). *Vegan: community ecology package. R package version 1.8-5*. Available at: http://www.cran.r-project.org.

Oliver, E. C. J., Burrows, M. T., Donat, M. G., Sen Gupta, A., Alexander, L. V., Perkins-Kirkpatrick, S. E., et al. (2019). Projected marine heatwaves in the 21st century and the potential for ecological impact. *Front. Mar. Sci.* 6. doi: 10.3389/fmars.2019.00734

Oliver, E. C. J., Donat, M. G., Burrows, M. T., Moore, P. J., Smale, D. A., Alexander, L. V., et al. (2018). Longer and more frequent marine heatwaves over the past century. *Nat. Commun.* 9, 1–12. doi: 10.1038/s41467-018-03732-9

Osman, E. O., Smith, D. J., Ziegler, M., Kürten, B., Conrad, C., El-Haddad, K. M., et al. (2018). Thermal refugia against coral bleaching throughout the northern Red Sea. *Glob. Change Biol.* 24, e474–e484. doi: 10.1111/gcb.13895

Petrou, K., Nunn, B. L., Padula, M. P., Miller, D. J., and Nielsen, D. A. (2021). Broad scale proteomic analysis of heat-destabilised symbiosis in the hard coral Acropora millepora. *Sci. Rep.* 11, 1–16. doi: 10.1038/s41598-021-98548-x

Pörtner, H. O., and Farrell, A. P. (2008). Ecology: Physiology and climate change. *Sci. (80-.).* 322, 690–692. doi: 10.1126/science.1163156

Rädecker, N., Pogoreutz, C., Gegner, H. M., Cárdenas, A., Roth, F., Bougoure, J., et al (2021). Heat stress destabilizes symbiotic nutrient cycling in corals. *Proc. Natl. Acad. Sci.* 118 (5), e2022653118. doi: 10.1073/pnas.2022653118

Ralph, P. J., and Gademann, R. (2005). Rapid light curves: A powerful tool to assess photosynthetic activity. *Aquat. Bot.* 82, 222–237. doi: 10.1016/j.aquabot.2005.02.006

R Core Team (2020). *R Core Team R: a language and environment for statistical computing* (Foundation for Statistical Computing).

Rodrigues, L. J., Grottoli, A. G., and Pease, T. K. (2008). Lipid class composition of bleached and recovering Porites compressa Dana 1846 and Montipora capitata Dana 1846 corals from Hawaii. *J. Exp. Mar. Bio. Ecol.* 358, 136–143. doi: 10.1016/j.jembe.2008.02.004

Sahin, D., Schoepf, V., Filbee-Dexter, K., Thomson, D., Radford, B., and Wernberg, T. (2023). Heating rate explains species-specific coral bleaching severity during a simulated marine heatwave. *Mar. Ecol. Prog. Ser.* 706, 33–46. doi: 10.3354/meps14246

Savary, R., Barshis, D. J., Voolstra, C. R., Cárdenas, A., Evensen, N. R., Banc-Prandi, G., et al. (2021). Fast and pervasive transcriptomic resilience and acclimation of extremely heat-tolerant coral holobionts from the northern Red Sea. *Proc. Natl. Acad. Sci. USA* 118 (19), e2023298118. doi: 10.1073/pnas.2023298118

Sawall, Y., Al-Sofyani, A., Hohn, S., Banguera-Hinestroza, E., Voolstra, C. R., and Wahl, M. (2015). Extensive phenotypic plasticity of a Red Sea coral over a strong latitudinal temperature gradient suggests limited acclimatization potential to warming. *Sci. Rep.* 5 (1), 8940. doi: 10.1038/srep08940

Sebastián, C. R., Sink, K. J., McClanahan, T. R., and Cowan, D. A. (2009). Bleaching response of corals and their Symbiodinium communities in southern Africa. *Mar. Biol.* 156, 2049–2062. doi: 10.1007/s00227-009-1236-8

Shlesinger, T., and van Woesik, R. (2023). Oceanic differences in coral-bleaching responses to marine heatwaves. *Sci. Total Environ.* 871, 162113. doi: 10.1016/j.scitotenv.2023.162113

Speare, K. E., Adam, T. C., Winslow, E. M., Lenihan, H. S., and Burkepile, D. E. (2022). Size-dependent mortality of corals during marine heatwave erodes recovery capacity of a coral reef. *Glob. Change Biol.* 28, 1342–1358. doi: 10.1111/gcb.16000

Spencer, T., Teleki, K. A., Bradshaw, C., and Spalding, M. D. (2000). Coral bleaching in the southern Seychelles during the 1997–1998 Indian Ocean warm event. *Mar. pollut. Bull.* 40, 569–586. doi: 10.1016/S0025-326X(00)00026-6

Szmant, A. M., and Gassman, N. J. (1990). The effects of prolonged "bleaching" on the tissue biomass and reproduction of the reef coral Montastrea annularis. *Coral Reefs* 8, 217–224. doi: 10.1007/BF00265014

Tremblay, P., Gori, A., Maguer, J. F., Hoogenboom, M., and Ferrier-Pagès, C. (2016). Heterotrophy promotes the re-establishment of photosynthate translocation in a symbiotic coral after heat stress. *Sci. Rep.* 6, 1–14. doi: 10.1038/srep38112

Veal, C. J., Carmi, M., Fine, M., and Hoegh-Guldberg, O. (2010). Increasing the accuracy of surface area estimation using single wax dipping of coral fragments. *Coral Reefs* 29, 893–897. doi: 10.1007/s00338-010-0647-9

Voolstra, C. R., Valenzuela, J. J., Turkarslan, S., Cárdenas, A., Hume, B. C. C., Perna, G., et al. (2021). Contrasting heat stress response patterns of coral holobionts across the Red Sea suggest distinct mechanisms of thermal tolerance. *Mol. Ecol.* 30, 4466–4480. doi: 10.1111/mec.16064

Warner, M. E., Fitt, W. K., and Schmidt, G. W. (1999). Damage to photosystem II in symbiotic dinoflagellates: A determinant of coral bleaching. *Proc. Natl. Acad. Sci. USA* 96, 8007–8012. doi: 10.1073/pnas.96.14.8007

Wickham, H. (2016). "ggplot2: elegant graphics for data analysis," in *ggplot2* (New York: Springer-Verlag), 189–201.

Ziegler, M., Roder, C. M., Büchel, C., and Voolstra, C. R. (2014). Limits to physiological plasticity of the coral Pocillopora verrucosa from the central Red Sea. *Coral Reefs* 33, 1115–1129. doi: 10.1007/s00338-014-1192-8

Zor, T., and Selinger, Z. (1996). Linearization of the Bradford protein assay increases its sensitivity: theoretical and experimental studies. *Anal. Biochem.* 236, 302–308. doi: 10.1006/abio.1996.0171